Fracture Mechanics of Concrete Structures,
Proceedings FRAMCOS-2, edited by Folker H. Wittmann,
AEDIFICATIO Publishers, D-79104 Freiburg (1995)

CRACK PROPAGATION IN CONCRETE SPECIMENS SUBJECTED TO SUSTAINED LOADS

A. Carpinteri, S. Valente and F. P. Zhou
Dept. of Structural Engineering, Politecnico di Torino, Torino, Italy
G. Ferrara and G. Melchiorri
ENEL-CRIS, Milano, Italy

Abstract

Three series of tensile and flexural creep tests on partially damaged concrete specimens are analyzed by means of the Time-Dependent Fictitious Crack Model. Each specimen was loaded to a given point in the softening branch and then unloaded. After that the specimen was reloaded to a certain percentage of the unloading start load (six levels from 70% to 95%) and then the sustained loading started.

The material constitutive laws in the model were derived from tensile tests. The model was applied to the simulation of two series of flexural tests, which produced load-deflection curves, creep deflection-time curves and sustained load level-failure time curves. A very satisfactory agreement between the experimental results and the theoretical simulations is achieved.

1 Introduction

Cracking is recognized as one of the important factors in creep of concrete structures. Therefore various crack models are adopted in creep analysis of concrete, e.g. Bazant (1985), de Borst (1986). However, time-independent crack models are usually utilized and only time-dependent deformations outside the fracture process zones are taken into account. In most cases it is justified to do so as sustained load levels are low and cracks grow to a limited extent.

At high sustained load levels, however, crack propagation may have a dominating influence on creep processes and eventually lead to failure [Mindess (1984), Wittmann (1984)]. In order to simulate creep crack growth and failure, the Time-Dependent Fictitious Crack Model has been developed and applied to analyze creep fracture of concrete in bending and compact tension tests by Zhou (1992).

During the last two decades more attention has been paid to the post-peak softening behavior of concrete structures under static loading. Recently, three series of tensile and flexural creep tests on concrete specimens already loaded to some point after peak-point were performed at ENEL-CRIS, Milan. The Time-Dependent Fictitious Crack Model was applied to the simulation of the tests. The main results are presented below and further details can be found in the internal report by Carpinteri et al. (1994).

2 Experiments

2.1 Testing program

The experimental program included tensile creep, flexural creep and fracture energy tests. The geometries and dimensions of the specimens are given in Table 1.

The mix proportion of the concrete is cement:water:sand:gravel = 480:230:825:825 kg/m^3. Portland cement type 425, alluvial sand (maximum size 3.15 mm) and gravel (maximum size 10 mm) were used.

In flexural creep tests, deflection was measured at the load application point as the mean value of two transducers (Fig. 1).

Table 1. Type of test and dimensions of specimens.

Type of test	No. of test	Specimen	Dimensions (mm)	Notch depth (mm)
Tensile creep	20	Notched cylinders	Φ100*200	10
Flexural creep Series I	18	Notched beams	840*100*100	20
Flexural creep Series II	22	Notched beams	840*100*100	20
Fracture energy	4	Notched beams	840*100*100	20

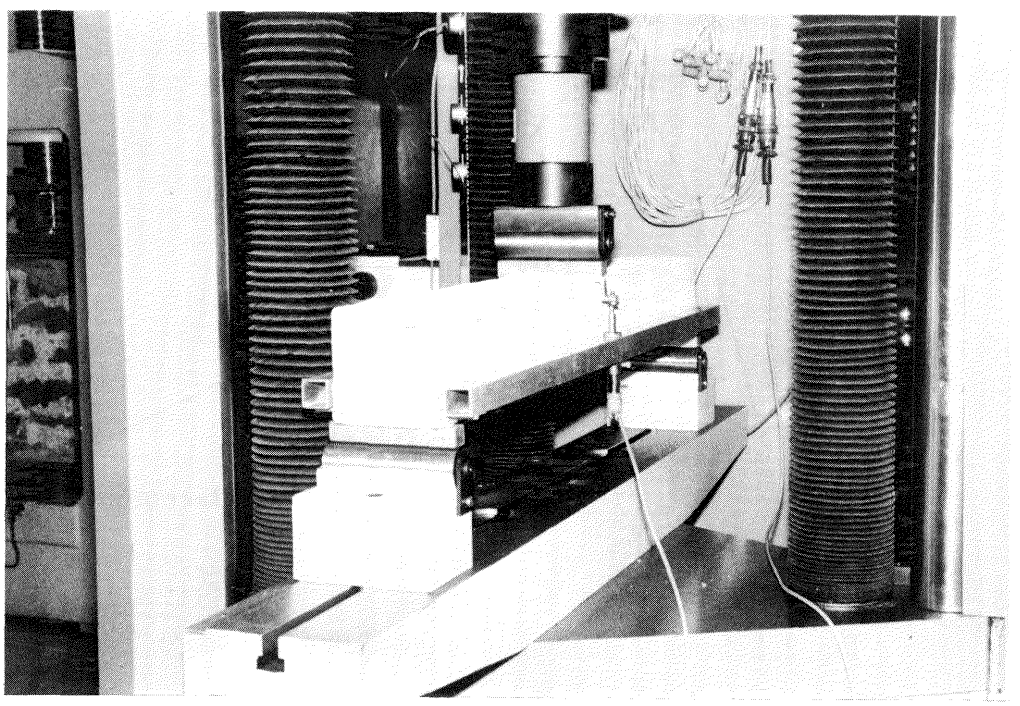

Fig. 1. Testing set-up.

2.2 Procedure of creep tests

The following steps (Fig. 2) are carried out in the creep tests.

1. Load up to the maximum load P_{max} with displacement control (0.2 $\mu m/s$).
2. Follow the softening branch until the load decreases to the prescribed value, P_D, i.e. unloading start load, (P_D = 7.84 kN in tensile tests; P_D = 1.18 kN in flexural test series I and P_D = 1.76 kN in flexural test series II).
3. Unload to about 10% of the maximum load, P_{max}.
4. Reload up to a load corresponding to a certain percentage of P_D, for each one of the six levels (i.e. 70%, 75%, 80%, 85%, 90% or 95% of P_D).
5. The load is held constant (± 4.9 kN) until creep failure occurs or steady creep stage is reached (i.e. creep rate is approximately zero).
6. After creep failure, the softening branch is followed if possible.

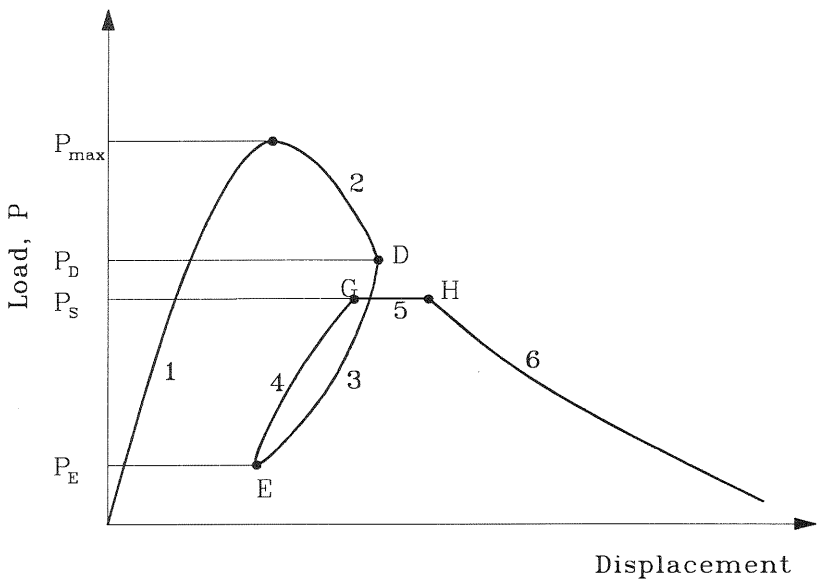

Fig. 2. Schematic illustration of the testing procedure.

3 Time-Dependent Fictitious Crack Model

The Time-Dependent Fictitious Crack Model developed by Zhou (1992) has been modified and used to analyze the experimental results. In this model the time-dependency is considered only in the fracture process zone, whereas the undamaged zone is assumed to be linear elastic.

A linear stress-strain relationship is used for the undamaged zone while the cohesive stress-COD (Crack Opening Displacement) law for the fracture process zone is illustrated in Fig. 3. The bilinear stress-COD curve proposed by Petersson (1981) is used as the envelope criterion for creep failure. This means that total COD increases from G to H when the stress is kept constant, and after the failure point H the static softening branch will be followed (i.e. segments HBC). The unloading path follows segment DE and the reloading path is EFG. Stiffness values are shown in Fig. 3.

The time-dependent stress-COD relationship is expressed in this model in an incremental form as:

$$d\sigma = d\sigma^R + F dw^I , \tag{1}$$

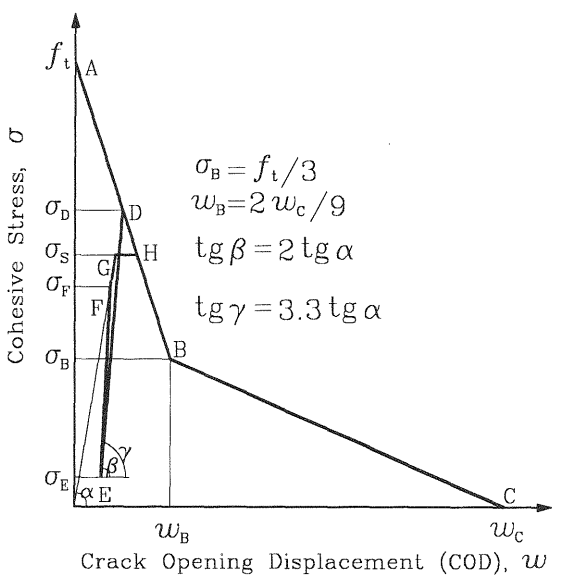

Fig. 3. Cohesive stress-COD law for the Time-Dependent Fictitious Crack Model; $tg\beta$ and $tg\gamma$ are slopes of the segments DE and FE respectively.

where $d\sigma^R$ and dw^I are the stress increments related to time increment dt, due to relaxation and COD respectively, and F is the reloading stiffness (the slope of FG in Fig. 3).

In the present analysis the stress increment due to relaxation is given by the expression:

$$d\sigma^R = -Fdw^C = -F\dot{w}^C dt, \tag{2}$$

where $\dot{w}^C$ is the creep rate as derived from the tensile creep tests (see Appendix A) and is expressed as:

$$\frac{\dot{w}^C}{w^C_{ult}} = 0.0096 * (\frac{\sigma_S}{\sigma_D})^{27} (0.556 + 10.2(\frac{w^C}{w^C_{ult}})^5 + 4.45\exp(-50\frac{w^C}{w^C_{ult}})). \tag{3}$$

The finite element program developed by Zhou (1992) has been used. Tensile strength, Young's modulus and fracture energy are 2.5 MPa, 38 GPa and 132 Nm/m^2, respectively. Tensile strength and fracture energy values were evaluated from tensile tests and fracture tests, respectively, while Young's modulus was evaluated from the mean load-deflection curve of four fracture energy tests, by best fitting the initial part of the curve numerically.

4 Results and comparisons

The two series of flexural creep tests were simulated by the model. The only difference between the two series is the load at the unloading start point. The unloading start load is 1.18 kN for series I and 1.76 kN for series II, respectively. Each series includes six sustained load levels, i.e. 70%, 75%, 80%, 85%, 90% and 95% of the unloading start load (the current load-carrying capacity).

The numerical results include load-deflection curves, creep deflection versus time curves and sustained load level versus failure time curves. Some typical results are presented below.

4.1 Load-deflection curves

The simulated load-deflection curves at two levels (90% and 80%) for each series are compared with the corresponding experimental ones in Figs. 4 and 5. In both cases the agreement is rather good. This is not surprising, as concerns the ascending part and the descending part down to the unloading start point, as the model is essentially identical to the FCM. What is necessary to comment is that the simulated softening parts after creep fracture agree well with the experiments. These considerations imply

that the descending part may be an appropriate envelope criterion for creep fracture.

(a)

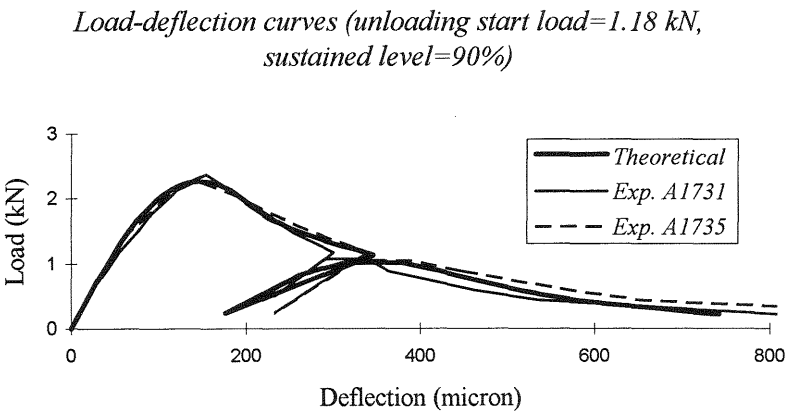

(b)

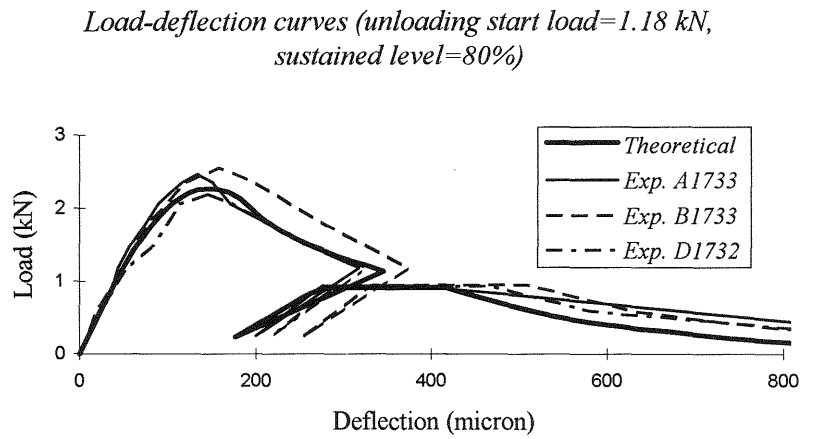

Fig. 4. Experimental and simulated load-deflection curves in flexural test series I; (a) sustained load level = 90%, (b) sustained load level = 80%.

(a)

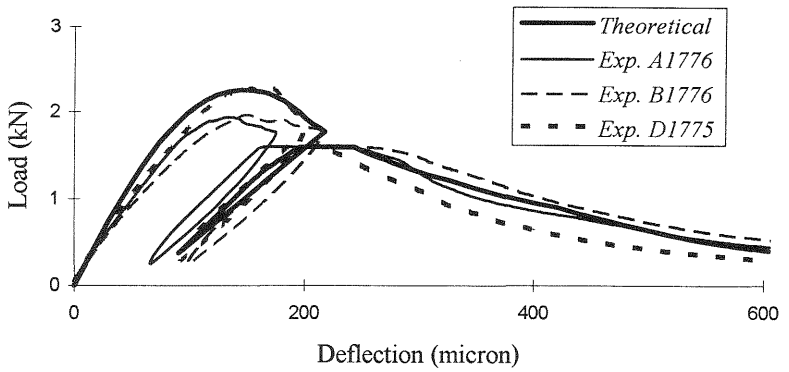

(b)

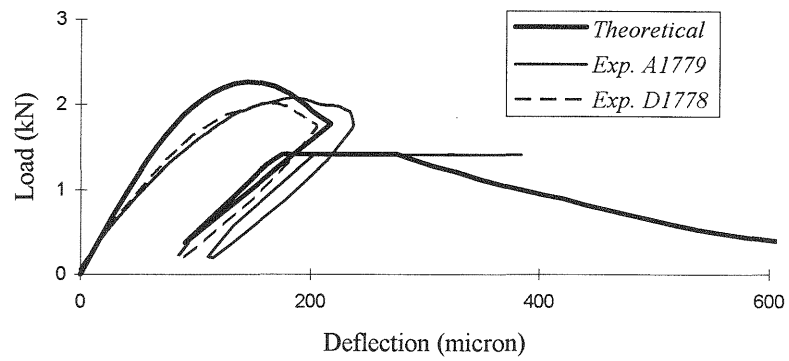

Fig. 5. Experimental and simulated load-deflection curves in flexural test series II; (a) sustained load level = 90%, (b) sustained load level = 80%.

4.2 Creep deflection versus time curves

Figs. 6 and 7 show some of the mean experimental and theoretical creep curves for the two series of flexural creep tests. Two sustained load levels (90% and 80%) for each series are included here.

The experimental creep curves display three stages as normally found in a complete creep test under high sustained loading. The primary stage starts

with a high creep rate and approaches the secondary stage when the rate tends to be almost constant. In the tertiary stage the creep rate increases rapidly up to failure. The primary and tertiary stages take up a small portion of the creep process, whereas the secondary stage covers the major part of failure lifetime. The model seems able to simulate the three-stage creep process.

(a)

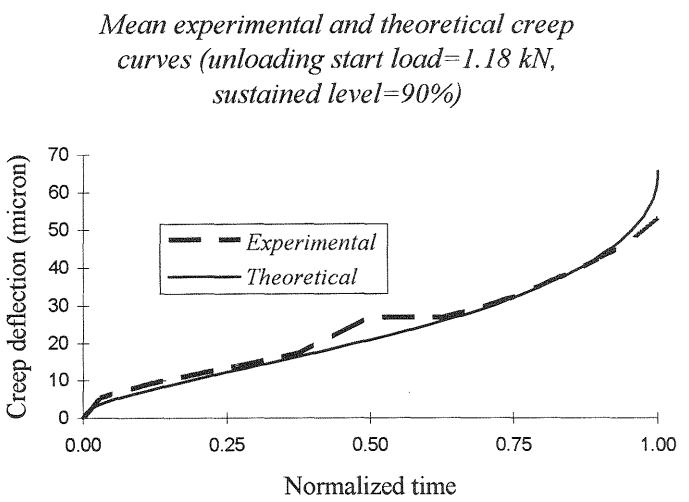

(b)

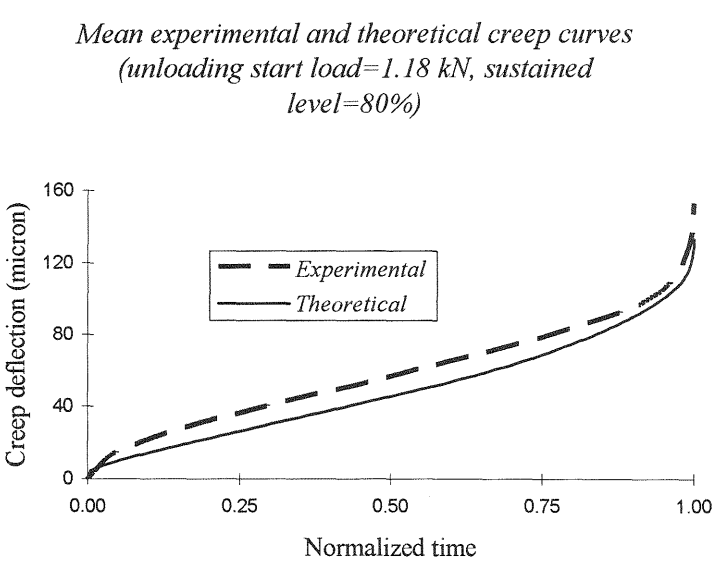

Fig. 6. Mean experimental and simulated creep curves for series I; (a) sustained load level =90%, (b) sustained load level = 80%.

(a)

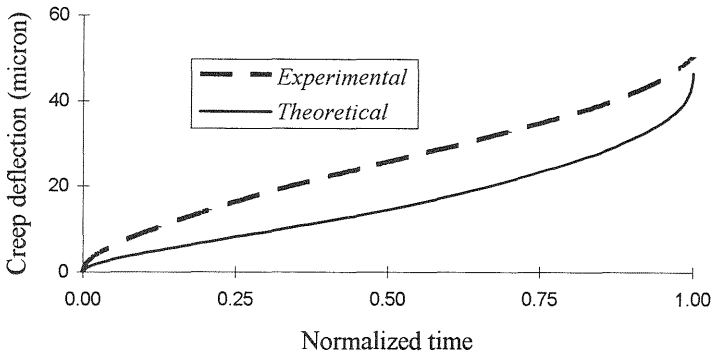

(b)

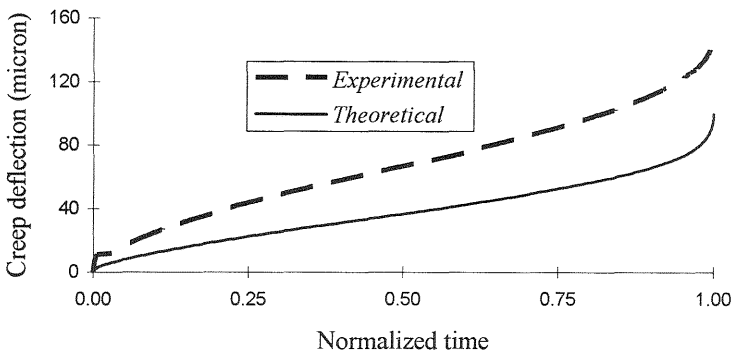

Fig. 7. Mean experimental and simulated creep curves for series II; (a) sustained load level = 90%, (b) sustained load level = 80%.

4.3 Sustained load level versus failure time curves

The simulated sustained load level versus failure time curves obtained for the two test series are shown in Fig. 8. The theoretical predictions agree fairly well with the experiments, except for level 95%.

The experiments indicate that, the level being the same, the failure time in series I is shorter than that in series II. In addition, the creep failure limit (i.e. the level below which no creep fracture occurs) for series I seems to be lower than that for series II. The only difference between the two series

is that the unloading start load in series I is lower than that in series II. The unloading start load may be regarded as the current load-carrying capacity. Therefore we may assert that the capability of resisting creep fracture decreases with the decrease in the current load-carrying capacity of a structure.

(a)

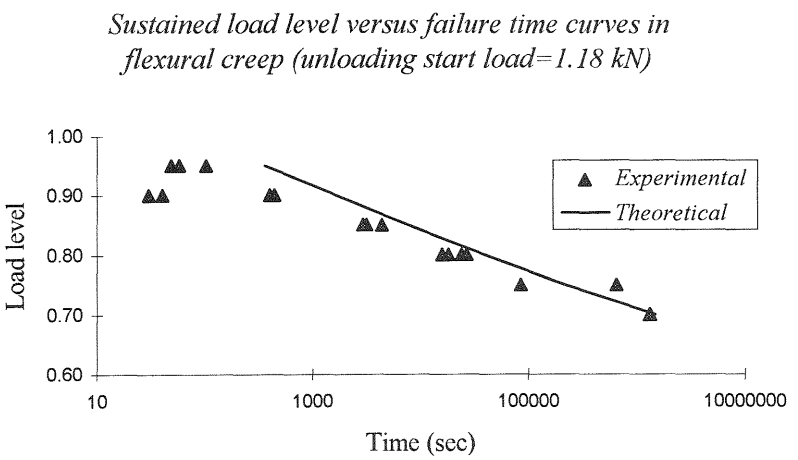

(b)

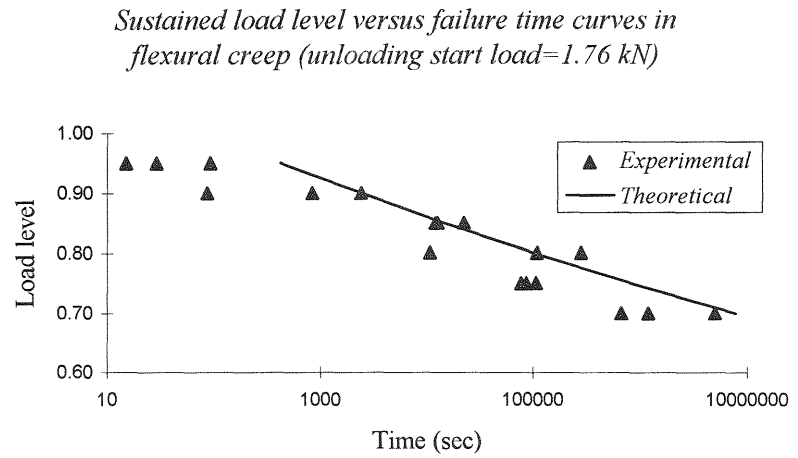

Fig. 8 Sustained load level versus failure time curves;
(a) series I, (b) series II.

5 Conclusions

Three series of tensile and flexural creep tests are analyzed through the Time-Dependent Fictitious Crack Model and the following conclusions may be drawn.

1. The experimental load-deflection curves, including unloading and reloading cycle and descending branch after creep fracture, are satisfactorily simulated. The descending part of the static load-deflection curve may serve as a valid envelope criterion for creep fracture.
2. The model predicts creep curves very similar to the experimental ones.
3. The predicted sustained load level versus failure time curves are in rather good agreement with the experimental ones, for both test series. It appears that the capability of resisting creep fracture under sustained loading also decreases as the current load-carrying capacity decreases.

6 Acknowledgments

This investigation was carried out under a contract between the Politecnico di Torino and ENEL-CRIS-Milano.

7 References

Bazant, Z.P. and Chern, J.-C. (1985) Strain softening with creep and exponential algorithm. **J. Eng. Mech. Div.,** 111, 391-415.

Carpinteri, A., Valente, S. and Zhou, F. P. (1994) Creep crack propagation in concrete structures subjected to constant loads. **Research Report, Contract,** A634/93, Dept. of Structural Engineering, Politecnico di Torino.

De Borst, R. and Van de Berg, P. (1986) Analysis of creep and cracking in concrete members, in **Creep and Shrinkage of Concrete: Mathematical Modelling** (ed Z.P. Bazant), 527-538.

Hillerborg, A, Modeer, M. and Petersson, P.E. (1976) Analysis of crack formation and crack growth in concrete by means of fracture mechanics and finite element. **Cem. & Concr. Res.**, 6, 773-781.

Mindess, S. (1984) Rate of loading effects on the fracture of cementitious materials, in **Application of Fracture Mechanics to Cementitious Composites** (ed S. P. Shah), Northwestern University, U.S.A., 617-636.

Petersson, P. E. (1981) Crack Growth and Development of Fracture Zones in Plain Concrete and Similar Materials. Doctoral Thesis, Report TVBM-1006, University of Lund, Sweden.

Wittman, F. H. (1984) Influence of time on crack formation and failure of concrete, in **Application of Fracture Mechanics to Cementitious Composites** (ed S. P. Shah), Northwestern University, U.S.A., 593-615.

Zhou, F.P. (1992) Time-dependent crack growth and fracture in concrete, Doctoral Thesis. Report TVBM-1011, University of Lund, Sweden.

Zhou, F.P.(1993) Cracking analysis and size effect in creep rupture of concrete, in **Creep and Shrinkage of Concrete** (eds Z.P. Bazant and I. Carol), E&FN Spon, 407-412.

Appendix A Creep law derived from tensile tests

The results of the tensile creep tests are summarized and a creep law is derived from the results.

Sustained load level is plotted versus failure time in Fig. A.1. The best fitting equation is found to be:

$$t_{cr} = 104(\frac{\sigma_S}{\sigma_D})^{-27}. \tag{A.1}$$

It is observed that the shape of creep curves is rather similar except for one case (85%), if the curves are plotted in terms of normalized creep COD and time (i.e. w^c / w^c_{ult} and t / t_{cr}) (Fig. A.2). Therefore a unique function may be assumed to exist between w^c / w^c_{ult} and t / t_{cr} , independent of stress level and it is obtained through best-fitting as:

$$\frac{w^c}{w^c_{ult}} = \Phi(\frac{t}{t_{cr}}) = 0.05 + 0.452(\frac{t}{t_{cr}}) + 0.341(\frac{t}{t_{cr}})^{10} - 0.057\exp(-50\frac{t}{t_{cr}}). \tag{A.2}$$

Thus, normalized creep COD rate can be expressed as a function of normalized creep COD:

$$d(\frac{w^c}{w^c_{ult}}) / d(\frac{t}{t_{cr}}) = \Phi'(\frac{t}{t_{cr}}) = \Phi'(\Phi^{-1}(\frac{w^c}{w^c_{ult}})) = \Omega(\frac{w^c}{w^c_{ult}}). \tag{A.3}$$

In the present computation, by best-fitting the tensile test curves through the least square method, the function $\Omega(\frac{w^c}{w^c_{ult}})$ is found to be:

$$d(\frac{w^c}{w^c_{ult}}) / d(\frac{t}{t_{cr}}) = \Omega(\frac{w^c}{w^c_{ult}}) = 0.556 + 10.2(\frac{w^c}{w^c_{ult}})^5 + 4.45\exp(-50\frac{w^c}{w^c_{ult}}). \tag{A.4}$$

Normalized creep rate can thus be expressed as:

$$\frac{\dot{w}^c}{w^c_{ult}} = \Omega(\frac{w^c}{w^c_{ult}}) / t_{cr} = 0.0096 * (\frac{\sigma_S}{\sigma_D})^{27} (0.556 + 10.2(\frac{w^c}{w^c_{ult}})^5 + 4.45\exp(-50\frac{w^c}{w^c_{ult}})). \quad (A.5)$$

Since the experimental curves in Fig. A.2 are not very smooth, it is difficult to evaluate the normalized creep COD rate directly from the curves. Therefore, this two-step approximation procedure has been used.

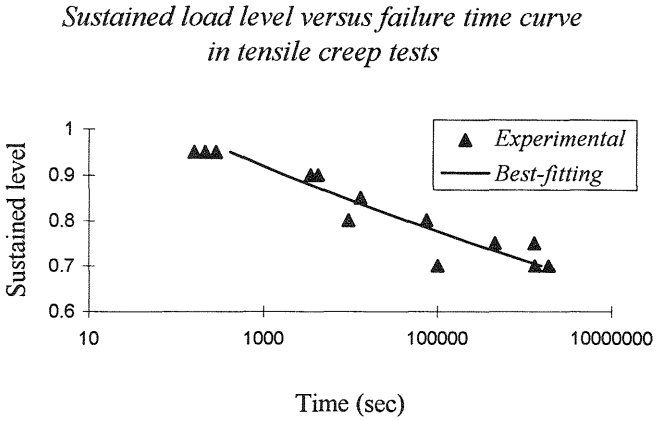

Fig. A.1 Sustained load level versus failure time curves in tensile creep tests.

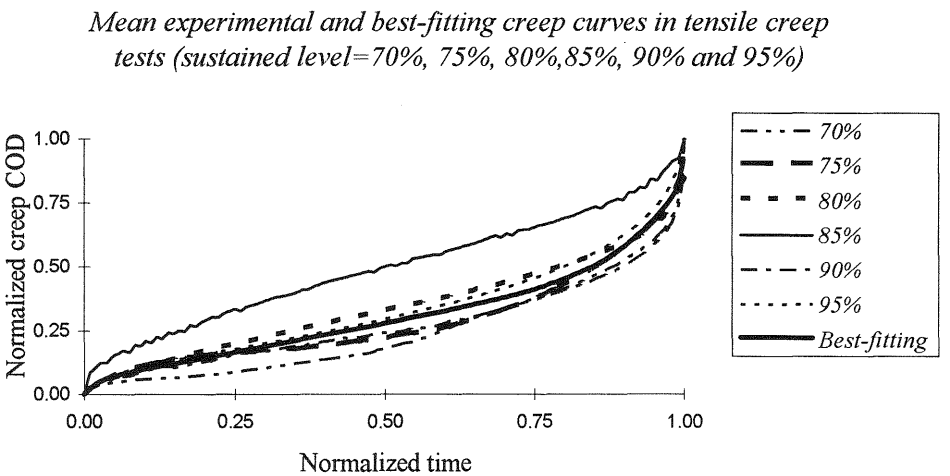

Fig. A.2 Mean experimental and best-fitting creep curves in tensile creep tests.